JOC Article

Nucleophilic Cyclopropane Ring Opening in Duocarmycin SA Derivatives by Methanol under Acid Conditions: A Quantum Mechanical Study in the Gas-Phase and in Solution

P. Cimino,[†,§] R. Improta,[†,‡] G. Bifulco,[§] R. Riccio,[§] L. Gomez-Paloma,*[,§] and V. Barone*[,†]

Dipartimento di Chimica, Università Federico II, Complesso Universitario Monte S.Angelo, via Cintia, I-80126 Napoli, Italy, and Dipartimento di Scienze Farmaceutiche, Università di Salerno, via Ponte don Melillo, 84084, Fisciano (SA), Italy

baronev@unina.it

Received November 14, 2003

We present a quantum-mechanical study of the S_N2 acid-catalyzed solvolysis with methanol of seven simplified duocarmycin SA (DNA alkylating agent) derivatives characterized by spirocyclic systems of increasing complexity, all containing the cyclopropyl/cyclohexadienone substrate. The reaction has been studied at the DFT-PBE0/6-31G(d) level in the gas phase and in methanol solution, using in the latter case the polarizable continuum model (PCM) to describe solvent effects. The results delivered by this computational protocol are in full agreement with the available experimental evidences and are not modified by extension of the basis set or by using a second-order many-body treatment (MP2) in place of DFT. This allows investigation of substituent effects in terms of structure/reactivity relationships and evaluation of the role of stereoelectronic effects. Furthermore, reactivity indices (hardness, electrophilicity) have been computed and shown to correlate well with activation energies. Together with their intrinsic interest, the details of the mechanism of the acid-catalyzed nucleophilic addition to the activated cyclopropane issuing from the present study pave the route for a deeper understanding of the molecular basis for the remarkable profile of the DNA-alkylation by DSA derivatives.

1. Introduction

Duocarmycin SA (DSA) and duocarmycin A (DA) are the parent members of a class of potent antitumor antibiotics related to CC-1065 (Figure 1) which deliver their biological activity through a sequence-selective alkylation of duplex DNA.[1−3] Extensive efforts have been devoted to defining the fundamental principles underlying the relationships between structure, chemical reactivity, and biological properties of these molecules. To this end, a number of deep-seated modifications in the agents[4−6] have been made, and their subsequent evaluation has provided important insights into the structural origin of their activity.

In the last years, several studies have defined the details of the DNA alkylation reaction which has been shown to proceed by a reversible, stereoelectronically controlled adenine N3 nucleophilic addition to the least substituted carbon atom of the cyclopropane ring within AT-rich minor groove regions of duplex DNA.[1] However, a definite structural basis for the origin of DNA catalysis for the reaction requires additional investigation.

With the aim of elucidating the most influential physicochemical factors in determining the reactivity of duocarmycins toward nucleophiles and, hopefully, of contributing to understand their unique selective DNA-sequence reactivity, a large variety of duocarmycin synthetic analogues has been extensively studied in solvolytic conditions.[7−10] The common structural characteristics of these ligands are a reactive cyclopropyl moiety, an indole ring, and an extended double-bond conjugation involving several rings and heteroatoms of the alkylating and binding subunits. These molecules show a remarkable chemical stability and need acidic catalysis for the addition of typical nucleophiles to take place onto the activated cyclopropane. This has led to the

[†] Dipartimento di Chimica.

[‡] Permanent address: Istituto di Biostrutture e Bioimmagini-CNR,M via Mezzocannone 6, I-80134 Napoli, Italy.

[§] Dipartimento di Scienze Farmaceutiche.

(1) Boger, D. L.; Johnson, D. L. *Angew. Chem., Int. Ed. Engl.* **1996**, *35*, 1438−1474.

(2) Boger, D. L.; Hertzog, D. L.; Bollinger B.; Johnson, D. L.; Cai H.; Goldberg, J.; Turnbull, P. *J. Am. Chem. Soc.* **1997**, *119*, 4977−4986.

(3) Boger, D. L.; Bollinger B.; Hertzog, D. L.; Johnson, D. L.; Cai H.; Mesini, P.; Garbaccio, R. M.; Jin, Q.; Kitos, P. A. *J. Am. Chem. Soc.* **1997**, *119*, 4987−4998.

(4) Baraldi, P. G.; Balboni, G.; Pavani, M. G.; Spalluto, G.; Tabrizi, M. A.; De Clercq, E.; Balzarini, J.; Bando, T.; Sugiyama, H.; Romagnoli, R. *J. Med. Chem.* **2001**, *44*, 2536−2543.

(5) Nagamura, S.; Asai, A.; Kobayashi, E.; Gomi, K.; Saito, H. *Bioorg. Med. Chem.* **1997**, *5*, 623−630.

(6) Amishiro, N.; Nagamura, S.; Kobayashi, E.; Okamoto, A.; Gomi, K.; Okabe, M.; Saito, H. *Bioorg. Med. Chem.* **2000**, *8*, 1637−1643.

(7) Boger, D. L.; Goldberg, J. A.; McKie, A. *Bioorg. Med. Chem. Lett.* **1996**, *6*, 1955−1960.

(8) Boger, D. L.; Santillan, A., Jr.; Searcey, M.; Jin, Q. *J. Org. Chem.* **1999**, *64*, 5241−5244.

(9) Boger, D. L.; Wysocki, Jr. R. J.; Ishizaki, T. *J. Am. Chem. Soc.* **1990**, *112*, 5230−5240.

(10) Boger, D. L.; Mesini, P. *J. Am. Chem. Soc.* **1994**, *116*, 11335−11348.

10.1021/jo0303517 CCC: $27.50 © 2004 American Chemical Society
Published on Web 03/23/2004

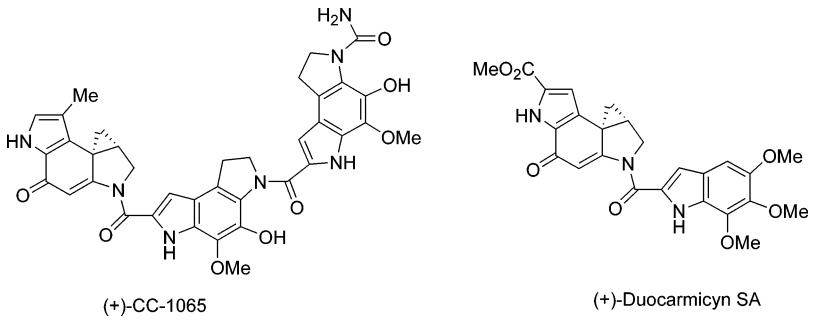

FIGURE 1. Structures of natural compounds (+)-CC-1065 and (+)-DSA.

assumption that the DNA alkylation can be an acid-catalyzed reaction.

Many studies provide strong evidence that the catalysis for the DNA alkylation reaction (pH 7.4) is derived from a DNA-binding-induced conformational change[11] in the agents that disrupts the conjugation activating the agents for pH-independent nucleophilic attack.[12−14]

Very useful hints have thus become available about the effect of variations in the molecular geometry on solvolytic reaction rates. However, due to the considerable complexity of the system, some mechanistic aspects are not yet well understood and the fine-tuning of the reactivity caused by different substituents on the DSA scaffold has not yet been fully interpreted.

In such a scenario, the recent advances of quantum mechanical methods based on the density functional theory (DFT)[15−16] allow one to treat systems of pharmacological and biological interest with an accuracy close to the "so-called" chemical accuracy. This could be very useful and, hopefully, will help one to gain a deeper insight into the molecular basis for the remarkable profile of the DNA alkylation by DSA derivatives.

As a first step in this direction, we decided to perform a detailed investigation of the S_N2-like acid-catalyzed solvolysis with methanol of seven simplified molecules characterized by spirocyclic systems of increasing complexity, all contaning the cyclopropyl/cyclohexadienone substrate (Figure 2). Herein, the density functional approach has been used to rationalize adequately the structure−reactivity relationships in terms of the role and of the effect of each moiety of the molecule on the reactivity of the duocarmycins.

To select and validate the most effective computational strategy we have investigated the reaction of the simplest spirocyclic derivative (**1**) in the gas phase and in solution. Next, we have analyzed the structure−reactivity relationships by comparing energetic, structural, and electronic parameters along the reaction paths of seven prototypical molecules. Finally, we have tried to interpret

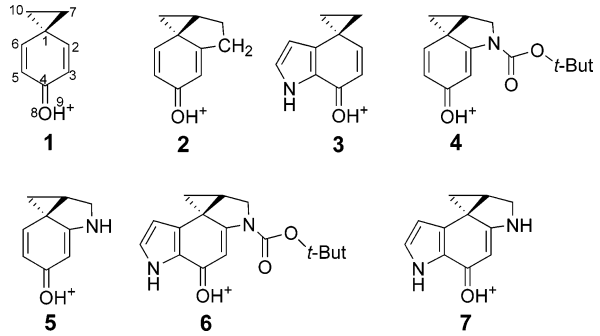

FIGURE 2. Structures of the model compounds analyzed in this study.

the relative reactivity of the seven compounds, in terms of electron-transfer, on the basis of the hardness (η_{DA}) and of the electrophilicity (ω) indices obtained by DFT calculations.

2. Methods

The calculations were carried out using the Gaussian 03 package.[17] In the gas phase, all structures were fully optimized and characterized as minima or transition states by calculating the harmonic vibrational frequencies at the PBE0/6-31G(d) level.[18] At these geometries, single-point energy evaluations were done at the PBE0/6-31G(d,p), PBE0/6-311+G(d,p), and MP2/6-311+G(d,p) levels.[19] Zero-point energies (ZPE's) and thermal contributions to thermodynamic functions and activation parameters were computed from the PBE0/6-31G(d) struc-

(11) Boger, D. L.; Santillan, A., Jr.; Searcey, M.; Jin, Q. *J. Am. Chem. Soc.* **1998**, *120*, 11554−11557.
(12) Boger, D. L.; Garbaccio, R. M. *J. Org. Chem.* **1999**, *64*, 5666−5669.
(13) Boger, D. L.; Boyce, C. W.; Johnson, D. L. *Bioorg. Med. Chem. Lett.* **1997**, *7*, 233−238.
(14) Ambroise, Y.; Boger, D. L. *Bioorg. Med. Chem. Lett.* **2002**, *12*, 303−306.
(15) Kock, W.; Holthousen, W. C. In A Chemist's Guide to Density Functional Theory; Wiley-VCH: Weinheim, 2000.
(16) Adamo, C.; Cossi, M.; Rega, N.; Barone, V. In *Theoretical Biochemistry: Processes and Properties of Biological Systems. Theoretical and Computational Chemistry*; Elsevier: New York, 2001; Vol. 9.

(17) Gaussian 03, Revision B.4: Frisch, M. J.; Trucks, G. W.; Schlegel, H. B.; Scuseria, G. E.; Robb, M. A.; Cheeseman, J. R.; Montgomery, J. A., Jr.; Vreven, T.; Kudin, K. N.; Burant, J. C.; Millam, J. M.; Iyengar, S. S.; Tomasi, J.; Barone, V.; Mennucci, B.; Cossi, M.; Scalmani, G.; Rega, N.; Petersson, G. A.; Nakatsuji, H.; Hada, M.; Ehara, M.; Toyota, K.; Fukuda, R.; Hasegawa, J.; Ishida, M.; Nakajima, T.; Honda, Y.; Kitao, O.; Nakai, H.; Klene, M.; Li, X.; Knox, J. E.; Hratchian, H. P.; Cross, J. B.; Adamo, C.; Jaramillo, J.;Gomperts, R.; Stratmann, R. E.; Yazyev, O.; Austin, A. J.; Cammi, R.; Pomelli, C.; Ochterski, J. W.; Ayala, P. Y.; Morokuma, K.; Voth, G. A.; Salvador, P.; Dannenberg, J. J.; Zakrewski, V. G.; Dapprich, S.; Daniels, A. D.; Strain, M. C.; Farkas, O.; Malick, D. K.; Rabuck, A. D.; Raghavachari, K.; Foresman, J. B.; Ortiz, J. V.; Cui, Q.; Baboul, A. G.; Clifford, S.; Cioslowski, J.; Stefanov, B. B.; Liu, G.; Liashenko, A.; Piskorz, P.; Komaromi, I.; Martin, R. L.; Fox, D. J.; Keith, T.; Al-Laham, M. A.; Peng, C. Y.; Nanayakkara, A.; Challacombe, M.; Gill, P. M. W.; Johnson, B.; Chen, W.; Wong, M. W.; Gonzalez, C.; Pople, J. A. Gaussian, Inc., Pittsburgh, PA, 2003.
(18) Adamo, C.; Barone, V. *J. Chem. Phys.* **1999**, *110*, 6158−6170.
(19) A description of basis sets and standard computational methods can be found in: Foresman, J. B.; Frisch, A. E. *Exploring Chemistry with Electronic Structure Methods*, 2nd ed.; Gaussian Inc.: Pittsburgh, PA, 1996.

tures and harmonic frequencies by using the rigid rotor/harmonic oscillator approximation and the standard expressions for an ideal gas in the canonical ensemble at 298.15 K and 1 atm.

Solvent effects have been taken into account via the self-consistent reaction field (SCRF) method using the polarizable continuum model (PCM).[20] In this method, the solvent is represented by an infinite dielectric medium characterized by the relative dielectric constant of the bulk (32.06 for CH_3OH at 298.15 K and 1 atm). Solvent effects have been estimated by single-point energy computations at the PBE0/6-31G(d) and PBE0/6-31G(d,p) levels. The reliability of this approximation has been checked by locating the transition state of compound **1** also in methanol solution at the PBE0/6-31G(d) level. We recall that the solvation energies issuing from PCM computations have the status of free energies, since they take implicitly into account thermal and entropic contributions of the solvent.[21]

The whole path for each reaction was traced by using the intrinsic reaction coordinate (IRC) at the PBE0/6-31G(d) level. The IRC calculation started from the optimized transition structure and followed the reaction path in both directions, toward the two minima it connects. We used up to 10 steps in each direction, with a step size of 0.3 $amu^{-1/2}$ bohr. Despite its limitations, the IRC[22] provides a very convenient description of reaction mechanisms as they are qualitatively treated by organic chemists.

The electronic structures were then analyzed by the natural bond orbital (NBO) model which allows one also to evaluate the stabilization energy connected to interactions between occupied orbitals of one reactant and empty orbitals of the second one.[23] Two reactivity descriptors were also computed, namely hardness (η) and electrophilicity index (ω). The former descriptor has been defined[24−27] as the difference between the vertical ionization energy (I) and electron affinity (A) of the neutral molecule, $\eta = I - A$, where

$$I = E(N = N_0 - 1) - E(\mathrm{N} = N_0) \text{ and } A = E(N = N_0) - E(N = N_0 + 1)$$

Here, N_0 is the number of electrons in the ground state of the (usually neutral) system. This necessitated the calculation of the energies of the neutral (N_0 electron system), cationic ($N_0 - 1$ electron system), and anionic ($N_0 + 1$ electron system) forms of each system. The electronegativity (χ) and the electronic chemical potential (μ) have been defined as $\chi = (I + A)/2 = -\mu$. The definition of the electrophilicity index (ω), given by Parr and co-workers,[24] is $\omega = \mu^2/2\eta$. Finally, the donor−acceptor intermolecular hardness (η_{DA}) is $\eta_{DA} = (I_D - A_A)$,

SCHEME 1. Schematic Diagram of the Solvolysis Reaction

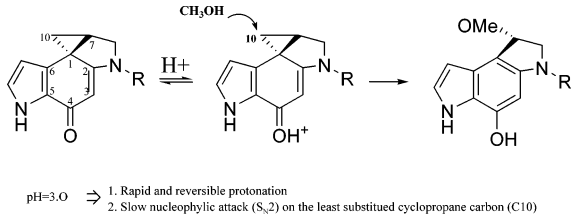

where A_A is the electron affinity of the acceptor A and I_D the vertical ionization energy of the donor molecule D.[28]

3. Results and Discussion

Before discussing our computational results, it is useful to summarize the most significant information on the title reaction obtained by previous experimental studies. The solvolysis (Scheme 1) occurs preferentially by cleavage of the C1−C10 bond with addition of a nucleophile to the least substitued C10 cyclopropane carbon versus cleavage of the C1−C7 bond with ring expansion and addition to C7.[7]

Furthermore, it has been established unambiguosly that the solvolysis of these molecules occurs with an addition of the nucleophile (CH_3OH) to the cyclopropane carbon (C10) through an S_N2 mechanism (Scheme 1), with clean inversion of the configuration at the reaction center.

The reaction is fully consistent with kinetic studies of the acid-catalyzed nucleophilic addition performed on related systems, where the reaction rate exhibits a first-order dependence on both the acid (pH) and the nucleophile concentration which is indicative of a mechanism involving rapid and reversible C4 carbonyl protonation followed by a slow, rate-determining S_N2 nucleophilic attack on the activated cyclopropane.[29]

On the basis of the analysis of several experimental data,[30−31] regarding the synthesis and the evaluation of the relative solvolytic rates of structural analogues (Figure 3), we established the following reactivity trends of the seven studied compounds (Figure 2):

1 > **2** > **5** > **7**; **1** > **3** > **6** > **7**; **1** > **4** > **5** > **7**; **1** > **4** > **6** > **7**

The relative reactivities of the duocarmycin derivatives, as established by their rate of acid-catalyzed solvolysis, are important in understanding the structural features underlying the chemical properties of these molecules. The direct comparison of two or more DSA analogues helps to define the role of the single portions of the natural molecule (DSA).

The experimental studies (Figure 3) proved that the half-life of **a′** is 35 s (pH = 3.0), whereas the simplest parent spiro[2.5]octa-1,4-dien-3one (**a**) undergoes rapid solvolysis of the cyclopropyl ring under acid conditions, the reduced reactivity reflecting the influence of the

(20) Cossi, M.; Rega, N.; Scalmani, G.; Barone, V. *J. Chem. Phys.* **2002**, *117*, 43−54.
(21) Tomasi, J.; Persico, M. *Chem. Rev.* **1994**, *94*, 2027.
(22) Gonzalez, C.; Schlegel, H. B. *J. Phys. Chem.* **1990**, *16*, 1170−1176.
(23) Reed, A. E.; Curtiss, L. A.; Weinhold, F. *Chem. Rev.* **1988**, *88*, 899−926.
(24) Parr, R. G.; Szentpaly, L.; Liu, S. *J. Am. Chem. Soc.* **1999**, *121*, 1922−1924.
(25) Chermette, H. *J. Comput. Chem.* **1999**, *20*, 129−154.
(26) Parr, R.; Pearson, R. G. *J. Am. Chem. Soc.* **1983**, *105*, 7512−7516.
(27) Pearson, R. G. *Chemical Hardness*; VCH: Weinheim, 1997.
(28) Ciofini, I.; Hazebroucq, S.; Joubert, L.; Adamo, C. *Theor. Chem. Acc.* **2004**, in press.
(29) Warpehoski, M. A.; Harper, D. E. *J. Am. Chem. Soc.* **1994**, *116*, 7573−7580.
(30) Boger, D. L.; Machiba, K.; Hertzog, D. L.; Kitos, P. A.; Holmes, D. *J. Am. Chem. Soc.* **1993**, *115*, 9025−9036.
(31) Boger, D. L.; Turnbull, P. *J. Org. Chem.* **1998**, *63*, 8004−8011.

TABLE 1. Energy Barrier with ($\Delta E_0^{\ddagger}$) and without ($\Delta E^{\ddagger}$) Zero-Point Contributions and Activation Parameters at Standard Conditions (298.15 K, 1 atm): Internal Energy ($\Delta U^{\ddagger}$), Enthalpy ($\Delta H^{\ddagger}$), and Free Energy ($\Delta G^{\ddagger}$) in the Gas Phase (PBEO/6-31G(d)) and in Solution (PCM-Solvent Model PBE0/6-31G(d)) for Compounds 1−7

	structure						
gas phase (PBE0/6-31G (d))	**1**	**2**	**3**	**4**	**5**	**6**	**7**
$\Delta E^{\ddagger}$ (kcal/mol)	-0.98	1.35	5.37	7.43	9.31	15.02	17.31
$\Delta E_0^{\ddagger}$ (kcal/mol)	-0.17	2.28	6.35	8.49	10.26	15.82	18.14
$\Delta U^{\ddagger}$ (kcal/mol)	0.36	2.77	6.82	8.95	10.67	16.43	18.63
$\Delta H^{\ddagger}$ (kcal/mol)	-0.24	2.18	6.22	8.35	10.07	15.83	18.04
$\Delta G^{\ddagger}$ (kcal/mol)	9.77	12.52	16.59	18.96	20.64	26.06	28.56

	structure						
solvent (PCM-PBE0/6-31G (d))	**1**	**2**	**3**	**4**	**5**	**6**	**7**
$\Delta G^{\ddagger}_{\text{without nonelectrostatic terms}}$ (kcal/mol)	4.69	5.36	9.60	6.23	12.50	12.07	18.87
$\Delta G^{\ddagger}_{\text{with nonelectrostatic terms}}$ (kcal/mol)	3.95	4.89	8.90	6.03	11.93	11.94	18.36

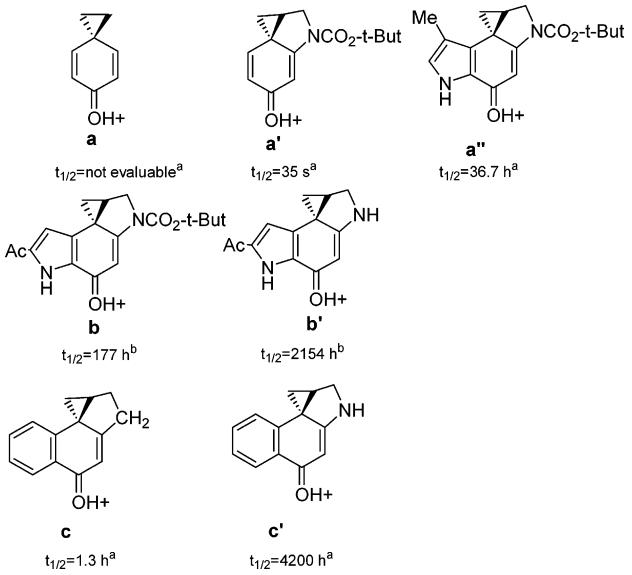

FIGURE 3. Comparative solvolytic rates of several synthetic analogues at pH = 3.0. Key: (a) 50% buffer−CH_3OH, buffer = (v/v/v) 4:1:20, 0.1 M citric acid, 0.2 M Na_2HPO_4, H_2O; (b) 50% buffer−CH_3OH, buffer = (v/v/v) 1:1:1, 0.1 M acetic acid, 0.2 M Na_2HPO_4, H_2O (25 °C).

flanking nitrogen heterocycle. Moreover, the comparison of **b** with **b′** reveals that **b** is more reactive, thus indicating the amide influence and the comparison of **a′** and **a″** is useful to establish the stabilizing effect of the pyrrole unit. Furthermore, a DSA derivative lacking the crucial nitrogen atom (**c**) was synthesized and was found to be exceptionally reactive, thus suggesting a nitrogen conjugative stabilization.

On the basis of this evidence, we selected the seven compounds (Figure 2) and established the reactivity trends consistent with the experimental results showed above. Indeed, the compounds **4** and **6** (Figure 2), bearing an *N*-acylating (*N*-CO_2-*t*-But) group, are more reactive of the compounds **5** and **7** (with NH): **4** > **5** and **6** > **7**. The pyrrole stabilizing effect is reflected as follows: **1** > **3**, **4** > **6** and **5** > **7**. Finally, the relative reactivity of **1** and **2** (**1** > **2**) and of **1** and **4** (**1** > **4**) reflects the presence of the flanking cycle, possibly including a nitrogen atom.

So, our purpose is to rationalize the structure−reactivity relationships with a comparative analysis of the geometries, the electronic structures, and the energies of the selected compounds.

To this end, we have evaluated the bare energy barriers $\Delta E^{\ddagger}$ (i.e., the electronic energy differences between TSs and the corresponding reactants), together with the corresponding free energies ($\Delta G^{\ddagger}$), which include zero-point, thermal, and entropic contributions (collectively referred to as nonpotential energy, NPE, terms). Table 1 shows that $\Delta E^{\ddagger}$'s and $\Delta G^{\ddagger}$ have parallel trends: as a consequence, the results will be presented in terms of free energies, which have a closer correspondence with experimental data, but the interpretation will be based on electronic contributions only.

To confirm the reliability of our computed data, we have also estimated the $\Delta G^{\ddagger}$ of the two compounds studied experimentally, **c** and **c′**, containing a benzene ring with respect to the structures **2** and **5** (Figure 3). Our results ($\Delta G^{\ddagger}$ = 17.8 and 28.6 kcal/mol for **c** and **c′**, respectively) are in full agreement with experimental data (solvolytic rates: **c** > **c′**, Figure 3).

3.1. Spiro[2.5]octa-1,4-dien-3-one. We started our study by characterizing the nucleophilic attack of a methanol molecule to the simplest and most reactive derivative of the duocarmycins, the spiro[2.5]octa-1,4-dien-3-one[32−33] (hereafter **1**, see Figure 2), which will be used as a reference system. Following the experimental indications, we have studied its protonated form, that one undergoing the substitution reaction.

PCM-PBE0/6-31G(d) calculations have been employed to locate and to characterize all the stationary points of the reaction path in methanol solution (see Figure 4). As expected, in the minimum energy structure of **1** (see Figure SI-1, Supporting Information), the protonation of O8 leads to a C4−O8 bond length (1.310 Å) slightly longer than in a standard dienone group (1.225 Å). At the same time, the C7−C10 bond acquires a partial double-bond character (bond distance 1.446 Å).

The NBO population analysis shows that the most important electronic interactions in **1** are those involving the cyclopropyl C1−C7 and C1−C10 bonds with the π^* orbitals of the C2−C3 and C5−C6 bonds. The σ CC bonds of cyclopropyl are less stable than normal σ bonds due to ring strain. They are thus closer in energy to the π^* orbitals of the dienone ring and their interaction with those orbitals is therefore particularly strong. This stabilization is made more effective by an orthogonal

(32) Baird, R.; Winstin, S. *J. Am. Chem. Soc.* **1962**, *85*, 567−578.
(33) del Rio, E.; Menendez, M. I.; Lopez, R.; Sordo, T. L. *J. Phys. Chem. A* **2000**, *104*, 5568−5571.

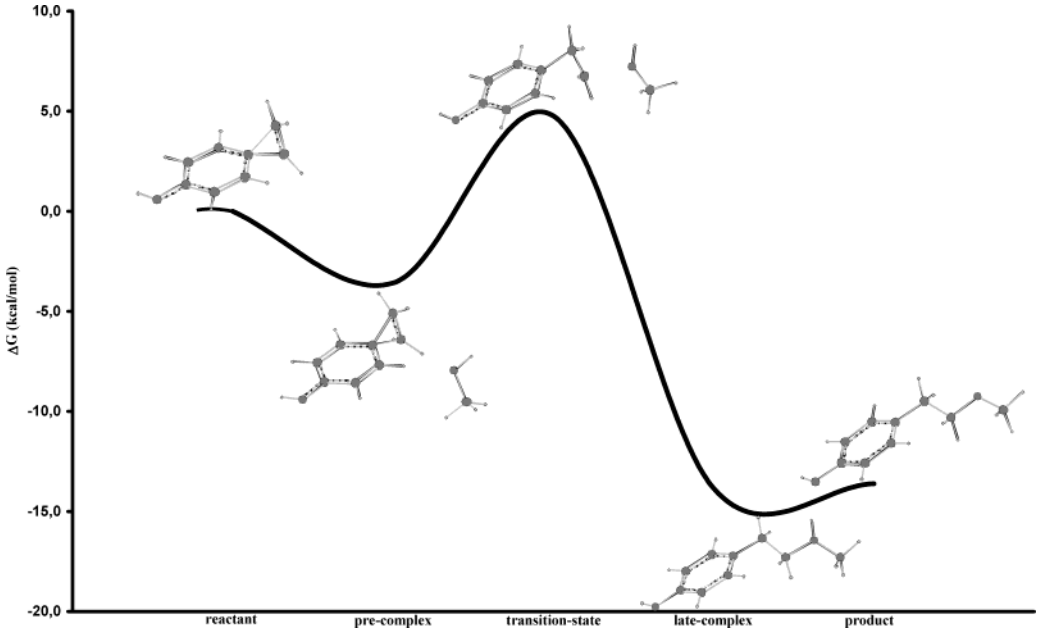

FIGURE 4. Reaction path of **1** in methanol solution (PCM-PBE0/6-31G(d)).

arrangement of the cyclopropyl moiety with respect to the dienone ring plane (Figure SI-1, Supporting Information), allowing the maximization of the electron conjugation between the two moieties (dihedral angles: $\alpha = 149.0°$, $\beta = -149.9°$, $\gamma = \delta = 0°$).

Inspection of the transition state (TS) governing the nucleophilic attack of the methanol molecule (**1-TS$_{solv}$**, Figure SI-1, Supporting Information) shows that, in full agreement with the experimental indications, the reaction consists of a concerted single step in which the bond-forming and -breaking processes occur almost simultaneously. In **1-TS$_{solv}$**, the C1−C10 bond distance is indeed lengthened up to 1.924 Å, the same order of magnitude of the incipient O_{Me}−C10 bond (2.147 Å). At the same time, in the dienone ring the C1−C2, C3−C4, C4−C5, and C1−C6 bond distances are shortened (1.415, 1.408, 1.407, 1.412 Å) and C2−C3 and C5−C6 distances are lengthened (1.376, 1.378 Å), mirroring the developing aromaticity. Finally, the C1−C7 bond is nearly coplanar ($\alpha = 175.5°$) to the ring, while the C1−C10 bond ($\beta = -132.0°$) shifts toward a more perpendicular arrangement.

Starting from the TS, IRC calculations show that the **1-TS$_{solv}$** structure converts to a precomplex, slightly stabilized with respect to separate reactants by a non conventional CH−O hydrogen bond, and a late complex between the reactants and the products, respectively (Figure 4).

The reaction rate of **1** reflects the stabilization of the S_N2 transition state through overlap between the adjacent π orbitals (C2−C3, C5−C6) and the p-type orbital which develops at the C1 atom in the transition state. The π system of this compound involves an extended conjugation (stabilization energy: p(C2−C3) to LP(C1) = 36.6 kcal/mol, Tables 4 and 5).

The computed free energy barrier is significantly lower in methanol solution than in the gas phase (4.5 vs 11.9 kcal/mol). The results of Table 1 show that nonelectrostatic solute−solvent interactions play a minor role, whereas the reduction of the free energy barrier is due to better electrostatic solute−solvent interactions for TSs than for reactants, which are, in turn, related to the increased polar character of TSs. The computed $\Delta G^{\ddagger}$ exhibit also a slight basis set dependence, their values increasing by ∼2 kcal/mol in vacuo and ∼0.5 kcal/mol in solution when going from the 6-31G(d) to the 6-311+G-(d,p) basis set (Figure 5). It is noteworthy that MP2/6-311+G(d,p) single-point calculations provide $\Delta G^{\ddagger}$ values close to those obtained at the PBE0 level, thus confirming the reliability of the adopted computational model.

Since geometry optimizations in solution are quite cumbersome, we next investigated if single-point PCM computations at geometries optimized in vacuo could provide sufficiently reliable values. Our results show that the solvent does not induce significant geometrical changes in the system **1** (Table 2, Figure SI-1 (Supporting Information), and Figure 6) and that energetic parameters (Table 3) obtained employing structures optimized in vacuo are very close to their counterparts issuing from geometry relaxation in solution. Consequently, we decided to evaluate solvent effects for the larger systems by single-point PCM calculations at the geometries optimized in the gas phase.

3.2. Spiro[2.5]octa-1,4-dien-3-one Derivatives. In the next step of our analysis, we characterized the acid-catalyzed solvolysis of duocarmycin derivatives **2**−**7** by methanol. For all the compounds examined, the reaction follows the same mechanism predicted for **1** (see Scheme 1). In agreement with the experimental data, the addition reaction, following an S_N2 mechanism, occurs at the less substituted carbon atom of the cyclopropane moiety. The structures of the stationary points are qualitatively similar to those computed for **1** but show some minor differences, related to the different reactivities.

As a matter of fact, a comparison of the $\Delta G^{\ddagger}$ of reaction for the seven compounds studied shows that the $\Delta G^{\ddagger}$ for **1** (the most reactive compound) is ∼20 kcal/mol lower

TABLE 2. Bond Lengths (in Å) and Mulliken Charges for the Compounds 1_{solv} and 1-TS_{solv} Optimized in Solution and 1−7 and 1-TS, 2-TS, 3-TS, 4-TS, 5-TS, 6-TS, and 7-TS in the Gas Phase (PBEO/6-31G(d))[a]

	structure							
	1_{Solv}	**1**	**2**	**3**	**4**	**5**	**6**	**7**
charge (*q*) on CH_2 group (carbon 10)	0.184	0.198	0.183	0.166	0.160	0.158	0.144	0.143
C1−C10	1.576	1.582	1.578	1.563	1.562	1.554	1.549	1.542

	structure							
	1-TS_{Solv}	**1-TS**	**2-TS**	**3-TS**	**4-TS**	**5-TS**	**6-TS**	**7-TS**
charge (*q*) on HO_{Me} group	−0.127	−0.138	−0.124	-0.112	−0.104	−0.102	−0.085	−0.083
C1-C10	1.925	1.984	2.021	2.058	2.070	2.077	2.124	2.132
C10-O_{Me}	2.147	2.068	1.999	1.948	1.897	1.887	1.809	1.801
Harmonic vibrational frequencies (cm^{-1})	339.9i	298.1i	316.3i	323.4i	356.4i	361.7i	357.0i	360.8i

[a] The Mulliken charges (*q*) refer to the $-CH_2-$ (for the carbon 10) and HO_{Me} groups. The harmonic vibrational frequencies refer to the transition vectors at the TSs.

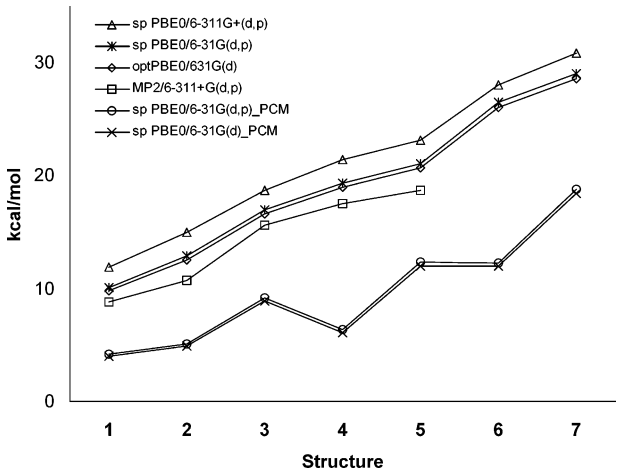

FIGURE 5. Activation free energies ($\Delta G^{\ddagger}$) for the compounds **1**−**7** in the gas-phase and in methanol solution. See the text for details.

than that of **7** (the least reactive). Our computations predict that:

1. The compounds bearing a pyrrole ring, **3**−**6**−**7**, display a relevant stability and a slower solvolytic rate with respect to **1**−**4**−**5**, respectively. The pyrrole effect increases the energy barriers ($\Delta G^{\ddagger}$ by ∼7 kcal/mol (in vacuo).

2. The presence of the fused five-membered rings on the structure **1** (cyclopentane and pyrrolidine) reduces the electrophilic reactivity of the C10 atom (smaller positive charge on C10 and shorter C1−C10 bond length). The calculated $\Delta G^{\ddagger}$ values provide a quantitative estimate of the reactivity order **1** > **2** > **5**.

3. *N*-Acylation (*N*-CO_2-*t*-But) increases the reaction rates of the compounds **4** and **6** with respect to the analogous compounds bearing an NH substituent (**5**, **7**), the computed $\Delta G^{\ddagger}$ decreasing by ∼2 kcal/mol (in vacuo).

All the above reactivity trends are in agreement with the experimental data. Inspection of Figure 5 shows that the computed energy barriers are significantly lower in methanol solution. A polar solvent strongly stabilizes indeed the transition states, which are significantly more polar than reactants and, as we will see later, decreases the gap between the HOMO of the nucleophile and the LUMO of the electrophile.

Solvent effects are similar for all the reactants examined ($\Delta G^{\ddagger}$ decreases by ∼6−10 kcal/mol) but not for **4** (∼13 kcal/mol) and **6** (∼14 kcal/mol), which exhibit a larger decrease. Since the solvation free energy of the corresponding transition states follows a trend similar to that of the remaining compounds, this result is probably due to a less effective solvation of the isolated reactants. This is not related to the presence of bulky *tert*-butyloxy groups since computations performed for the corresponding methyl analogues give comparable results. On the other hand, the particularly high positive charge of the protonated dienone in **4** and **6** (vide infra) could play a significant role. In particular, it cannot be excluded that a continuum solvent model is not able to describe with sufficient accuracy compounds with a localized positive charge, and thus, for those compounds, inclusion of the first shell solvent molecules might be mandatory. However, it is worth noting that the computed reactivity trend in solution agrees with the experimental one also for **4** and **6**.

In summary, the predictions of our computations are completely in line with the available experimental indications. In the following paragraphs, we will try to explain the physicochemical effects responsible for the different reactivities of the compounds examined. To this end, we will first present a comparative analysis of the structural and electronic properties of the seven isolated structures and of the respective transition states. In a second step, we will interpret the reactivity trends using different reactivity indexes.

As shown in Figure 5, the predicted trend is the same irrespective of the employed basis set, with $\Delta G^{\ddagger}$ increasing with the basis set size for all the seven compounds studied. Furthermore, the trend obtained at the MP2/6-311+G(d,p) level is nearly parallel to its PBE0/6-311G+-(d,p) counterpart, being shifted almost uniformly by 3 kcal/mol, thus indicating that the most significant computational results do not depend on the level of theory adopted. For this reason, the following discussion will be based essentially on the data obtained at the PBE0/6-31G(d) level.

3.3. Phsicochemical Effects Influencing the Reactivity. A comparative analysis of the geometry and electronic structure of the seven reactants under study shows some key fatures that can be nicely correlated to their different reactivity toward nucleophilic substitution. For instance, the C1−C10 bond length (Table 2, Figure SI-2, Supporting Information) and the positive charge on

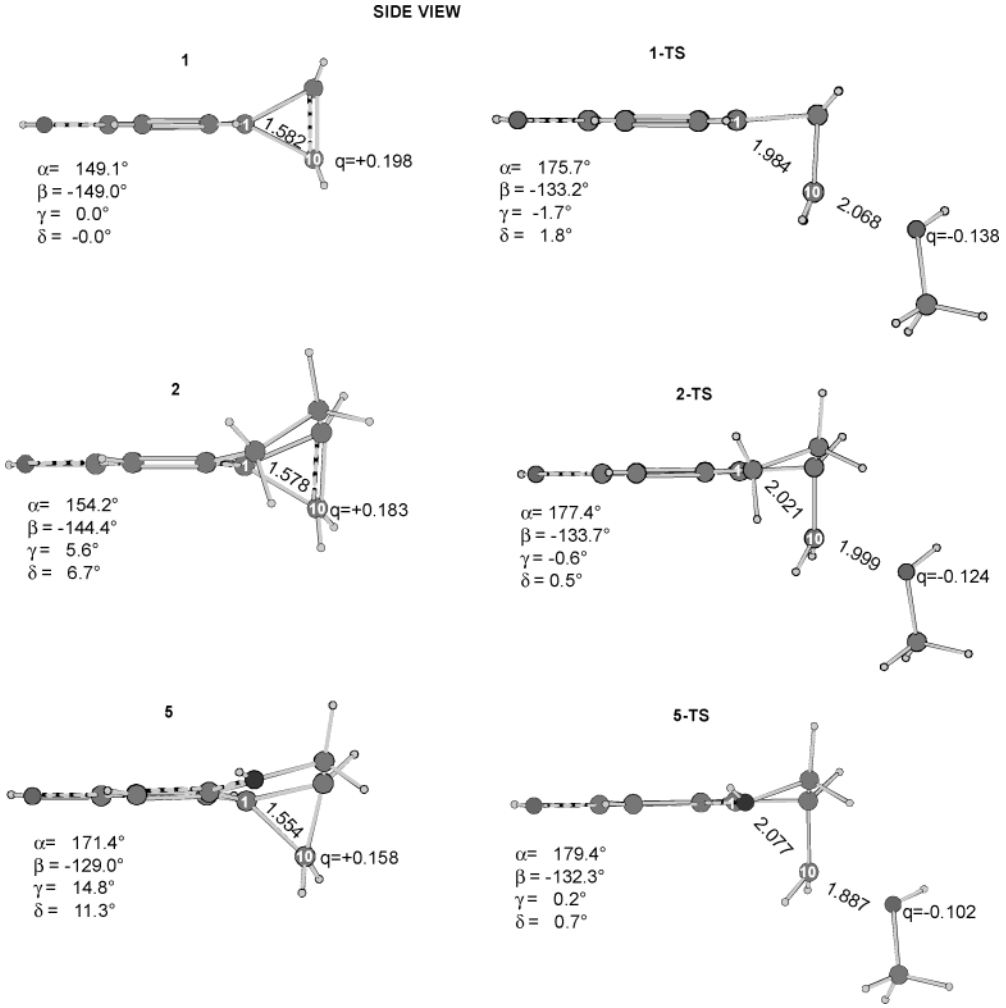

FIGURE 6. Side view of the structures **1**, **2**, and **5** and of the respective transition state in the gas-phase (PBE0/6-31G(d)). The bond lengths are in Å and the Mulliken charges (*q*) refer to the groups $-CH_2-$ (including C10) and HO_{Me}.

TABLE 3. Comparison between the Free Energies Computed by Full Optimization of the Structure 1 in Methanol Solution and the Free Energies Obtained by Single-Point Energy Evaluation on the Geometries Optimized in the Gas Phase

structure **1**	optimization PBE0/6-31G(d)	single-point PBE0/6-31G(d)
$\Delta G^{\ddagger}$(*TS*-react) (kcal/mol)	4.77	4.69
ΔG (precomple-react) (kcal/mol)	−3.58	−3.50
ΔG (products-react) (kcal/mol)	−13.61	−13.22
ΔG (late complex-react) (kcal/mol)	−13.84	−12.73

C10 carbon (Table 2, Figure SI-3) decrease on going from **1** to **7**.

As we have seen above, the protonation of the dienone oxygen atom leads to an increase of the aromatic character of the dienone and to a delocalization of the positive charge within the whole molecule. The former effect leads to a weakening of the C1−C10 bond (the C1−C2 and C1−C6 bonds acquire indeed a partial double bond character), whereas the latter effect causes an increase of the electrophilic character of the cylopropyl carbon atoms. Moreover, both effects favor the nucleophilic substitution of the methanol molecule. As a consequence, any substituent decreasing the aromaticity of the dienone ring and/or the delocalization of the positive charge in the cyclopropyl moiety leads to a larger reaction barrier. These features are mirrored in the transition-state structures. As a matter of fact, the "reactant like" character of transition state decreases when going from **1** to **7**: the C10−O bond distance decreases, whereas the C1−C10 bond distance increases (Table 2, Figure SI-2 and SI-3, Supporting Information). The less electrophilic character of the C10 atom due to the presence of the substituents makes more difficult the nucleophilic attack by the methanol molecule that is forced to get closer to the cyclopropyl moiety (Table 2). Within this general scheme it is then possible to analyze in deeper detail the role played by the different nature of the substituents examined.

Pyrrole. In line with the experimental results, our computations predict that a pyrrole substituent decreases the reactivity of **3** relative to the reference compound (**1**), both in the gas phase ($\Delta G^{\ddagger}$ = 16.6 vs 9.8 kcal/mol) and in methanol solution ($\Delta G^{\ddagger}$ = 8.9 vs 3.9 kcal/mol). This result is due to the conjugative effect of the pyrrole ring, resulting in a partial delocalization of the positive charge on the aromatic system within the pyrrole moiety. This leads to a significant decrease of the positive charge on C10 (from 0.198 to 0.166), and a decrease of the C1−C10 bond length (from 1.582 to 1.563 Å).

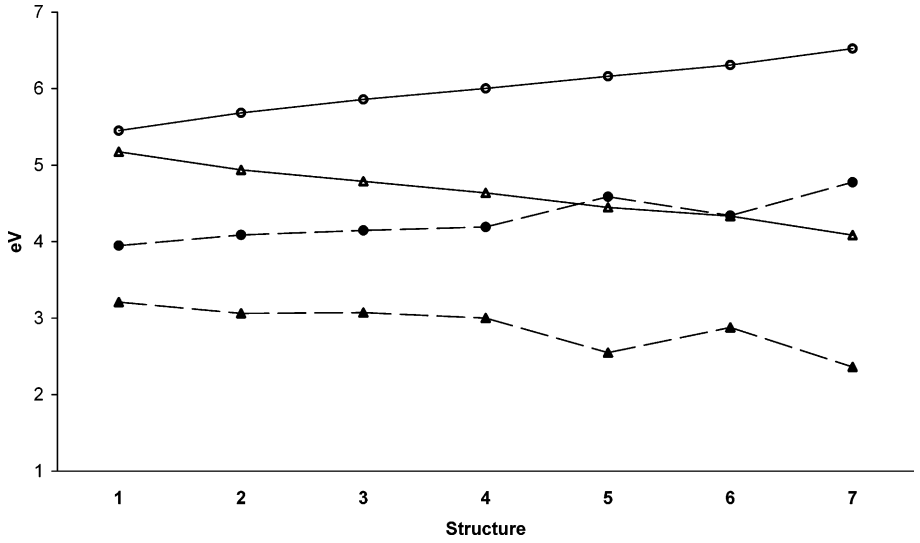

FIGURE 7. Reactivity indices: electrophilicity (ω, triangles) and hardness (η, circles) for compounds **1**−**7** in the gas phase (empty symbols) and in methanol solution (filled symbols). See the text for details.

Flanking Cycle. Compound **2** (Figure 6), in which the cyclopropane ring is locked into an orientation that prevents a perpendicular arrangement, reacts more slowly than compound **1**. The distortion of the planar conformation of the dienone, due to the flanking cycle, and the consequent reduced conjugation can explain the lower reactivity of this compound toward an S_N2 attack by methanol ($\Delta G^{\ddagger}$ = 12.5 vs 9.8 kcal/mol in the gas phase and 4.9 vs 3.9 kcal/mol in solution for **2** and **1**, respectively).

Indeed, the dihedral angles (Figure 6) reveal that the C1 atom is out of the plane (γ = 5.6°, δ = 6.7°) and that the C1−C7 and C1−C10 bonds shift down (α = 154.2°, β = −144.4°) with a resulting skew arrangement of the cyclopropyl ring with respect to the dienone plane. The NBO analysis allows us to put the above considerations on firmer ground. As a matter of fact, the stabilization energy for the C1−C7 (σ)/C2−C3 (π*) interaction and the s character of the C1 atom are lower in **2** than in **1** (see Table 4). This result suggests a less effective conjugation in the dienone ring, explaining the smaller positive charge on the C10 atom, q = +0.183 (Figure SI-2, Supporting Information) and the smaller reactivity of **2** toward a nucleophilic attack (Figure 5).

Moreover, the structural investigation of the transition state **2-TS** reveals a near coplanarity of the C1−C7 bond (α = 177.4°) with the dienone ring, an increase of the C1−C10 distance (2.021 vs 1.984 Å), and a decrease of the O_{Me}−C10 distance (1.999 vs 2.068 Å) with respect to **1-TS**, which is a clear answer to the greater difficulty by the methanol to react. The NBO analysis of the transition state **2-TS** leads to the same conclusions: indeed the structure shows how the lower reactivity of compound **2** reflects the reduced stabilization of the S_N2 transition state through overlap between the adjacent π orbitals (C2−C3, C5−C6) and the p-type orbital which develops at the C1 carbon in the transition state (p(C2−C3) to LP-(C1) = 35.0 kcal/mol, Tables 4 and 5).

Flanking Nitrogen Heterocycle. Our computations predict that a flanking nitrogen heterocycle leads to a decrease in the reactivity larger than that caused by a cyclopentane group ($\Delta G^{\ddagger}$ = 20.6 vs 12.5 kcal/mol in the gas phase and 11.9 vs 4.9 kcal/mol in solution for **5** and **2**, respectively). As a matter of fact, in **5** the dienone moiety is more distorted than in **2** (dihedral angles: α = 171.4 vs 154.2°, β = −129.0 vs −144.4°, γ = 14.8 vs 5.6°, δ = 11.3 vs 6.7°, Figure 6). Moreover, the presence of an electron donor group (the nitrogen atom) allows the delocalization of the positive charge of the dienone ring within the flanking cycle, with a consequent reduction of the positive charge on C10 (q = +0.158 vs +0.198) and, thus, of its reactivity toward methanol. The reactivity is related to a transition state structure with an oxygen atom closer to the electrophilic carbon (O_{Me}−C10 distance = 1.887 Å). Also in this transition state the C1−C7 bond is coplanar with the aromatic ring (α = 179.42°) and the

TABLE 4. Natural Hybrid Orbitals for the structures 1, 2, and 5

molecule	bond	center	% natural hybrid p character
1	C1C7(σ)	C1	82.5 ($sp^{4.74}$)
	C1C2(σ)	C1	67.4 ($sp^{2.07}$)
	C2C3(σ)	C2	63.5 ($sp^{1.74}$)
	C2C3(π)	C2	100.0 (p)
2	C1C7(σ)	C1	82.9 ($sp^{4.86}$)
	C1C2(σ)	C1	68.3 ($sp^{2.16}$)
	C2C3(σ)	C2	63.1 ($sp^{1.71}$)
	C2C3(π)	C2	100.0 (p)
5	C1C7(σ)	C1	82.6 ($sp^{4.76}$)
	C1C2(σ)	C1	71.2 ($sp^{2.47}$)
	C2C3(σ)	C2	61.4 ($sp^{1.59}$)
	C2C3(π)	C2	–

transition state	bond	center	% natural hybrid p character
1-TS	C1C7(σ)	C1	71.4 ($sp^{2.50}$)
	C1C2(σ)	C1	65.3 ($sp^{1.88}$)
	C2C3(σ)	C2	64.0 ($sp^{1.78}$)
	C2C3(π)	C2	100.0 (p)
2-TS	C1C7(σ)	C1	71.6 ($sp^{2.53}$)
	C1C2(σ)	C1	66.9 ($sp^{2.03}$)
	C2C3(σ)	C2	63.4 ($sp^{1.74}$)
	C2C3(π)	C2	99.94 ($sp^{99.99}d^{2.54}$)
5-TS	C1C7(σ)	C1	70.9($sp^{2.44}$)
	C1C2(σ)	C1	68.5 ($sp^{2.18}$)
	C2C3(σ)	C2	61.5 ($sp^{1.60}$)
	C2C3(π)	C2	99.93 ($sp^{99.99}d^{1.24}$)

TABLE 5. Stabilzation Energies (E(2)) for the molecules 1, 2, and 5

molecule	donor−acceptor	$E(2)$ (kcal/mol)
1	sp_{C1C7} to π^*_{C2C3}	5.8
	p_{C2C3} to σ^*_{C1C7}	3.6
2	sp_{C1C7} to π^*_{C2C3}	4.5
	p_{C2C3} to σ^*_{C1C7}	3.7
5	sp_{C1C7} to π^*_{C2C3}	−
	p_{C2C3} to σ^*_{C1C7}	−

transition state	donor−acceptor	$E(2)$ (kcal/mol)
1-TS	p_{C2C3} to LP_{C1}	36.6
2-TS	p_{C2C3} to LP_{C1}	35.0
5-TS	p_{C2C3} to LP_{C1}	32.7

C1−C10 distance is longer (2.077 Å), confirming that the driving force of the reaction is the aromaticity.

The analysis of the behavior of **4**, where the flanking cycle has an amide substituent, confirms the above considerations. In this compound, the nitrogen lone pair interacts with the CO group, as depicted in the "classical" amide resonance structure. As a consequence, it is less effective in delocalizing the positive charge on the dienone moiety. It is thus not surprising that **4** is more reactive than **5** ($\Delta G^{\ddagger} = 19.0$ vs 20.6 kcal/mol in the gas phase and 6.0 vs 11.9 kcal/mol in solution).

3.4. Analysis of the Computed "Reactivity Indices". Finally, we have checked if the most commonly used reactivity indices can be profitably employed for analyzing the reaction under study. We have selected, in particular, the electrophilicity ω (intramolecular parameter that depends only on the electronic characteristics of the acceptor species) and the donor−acceptor hardness η_{DA} (intermolecular parameter).

The ω index quantifies the tendency of a molecule to "soak up" electrons; thus, a high value corresponds to a great ability of the system to attract electron from a generic donor molecule. On the other hand, small values of the hardness η_{DA} indicate a strong interaction between donor and acceptor species, since this corresponds to a small energy gap between the donor HOMO and the acceptor LUMO. Although both indexes should give the same trend in vacuo since we are always considering the same nucleophile, this is no longer true when comparing gas phase and aqueous solution results since solvent effects can be different for the electrophile and the nucleophile.

Inspection of Figure 7 shows that calculated values for both ω and η have the same trend as the computed and experimental relative reactivities. As we have seen above, the reaction is predicted to be easier in methanol solution than in the gas phase. As a matter of fact, although solvent effects decrease the electrophilicity, they lead to a remarkable reduction of the η_{DA} values. Our calculations thus predict that a polar solvent reduces the intermolecular HOMO−LUMO energy gap, making easier transferring electrons from the donor to the acceptor.

4. Concluding Remarks

In the quantum mechanical study hereby presented we have analyzed, both in the gas phase and in methanol solution, the reaction between methanol and seven duocarmycin analogues in their protonated form. The scenario sketched by our computations is fully consistent with the available experimental indications: the nucleophile attack occurs at the least substituted carbon atom of the cyclopropyl ring, according to a S_N2 mechanism. A comparison between the activation free energies computed for the seven reactants provide a computational reactivity scale in full agreement with the experimental one. As a matter of fact, an examination of the seven structures established that the presence of the pyrrole ring, of the flanking cyclopentane and of the flanking nitrogen heterocycle conveys a stabilization to the compound **1**, reducing the solvolytic reactivity. These effects are related both to the electronic nature of the substituents and to steric effects.

Those results confirm the reliability of our computational model and, consequently, support the validity of all the qualitative considerations based on it. A synoptical analysis of the reaction paths for the seven compounds allows to highlight the physicochemical effects accounting for the different reactivity of the corresponding substrates. In short, the two key factors are the "degree of aromaticity" of the dienone ring and the amount of partial positive charge localized on the cyclopropyl carbon atom undergoing the nucleophile attack. The most the dienone ring acquires a phenol-like electronic structure, the most the C1−C10 bond is weakened, and thus, the easiest is the methanol attack. At the same time, the electrophilicity of C10 increases with its positive charge. The above considerations allow to explain the effect on the reaction rate not only of the substituents but also of the pH lowering. The protonation of the dienone oxygen increases both the aromaticty of the ring and the positive charge present on the cyclopropyl moiety.

The present study shows that a good relationship exists between the reactivity indices (η and ω) issuing from PBE0 calculations and the experimental reactivity order of the S_N2 reaction. This result is encouraging for a more thorough use of these properties for predicting the effect of suitable chemical modifications on the reactivity of duocarmycin derivatives.

From a methodological point of view, this study supports the usefulness of a theoretical investigation for the design of new and more effective compounds, highlighting the necessity of taking solvent effects in the proper account. As examplified by the large decrease in the activation energy due to the presence of the solvent, only a suitable treatment of environmental effects allows a semiquantitative and, hopefully, quantitative agreement between computations and experiments. Thus, besides providing deeper insight on the structure/reactivity relationships and on mechanistic aspects, the results hereby presented pave the route for the study of the interaction between duocarmycins and DNA. Continued work is in progress in our laboratories.

Acknowledgment. We thank the Italian Ministry of University and Research (MIUR) and Gaussian, Inc., for financial support.

Supporting Information Available: Figures SI-1, SI-2, and SI-3. *Z*-Matrixes, computed energies, imaginary frequencies, and thermodinamic data for all optimized structures **1**−**7** and corresponding precomplexes, transition-state structures, late complexes, and products. This material is available free of charge via the Internet at http://pubs.acs.org.

JO0303517